Field Simulation of Applicators for Interstitial Microwave Hyperthermia

G. Schaller, J. Erb, R. Engelbrecht, H.M. Seegenschmiedt.

Laboratories for High Frequency Technology (LHFT),
University Erlangen - Nürnberg, Cauerstraße 9, 91058 Erlangen, Germany.

ABSTRACT

The electromagnetic field near clinically applied coaxial microwave applicators for interstitial hyperthermia is calculated using a finite integration algorithm program. Simulations of E-field and SAR distributions of different conventional applicators in a muscle phantom are presented and compared with measurements.
The applied calculation method allows also design optimization and improvement of more sophisticated applicator types, e.g. those using a triaxial technique.

INTRODUCTION

More than a decade ago, it has become apparent that the use of microwave and radio-frequency applicators is a reliable method for effective heating of malignant tumors [1]. Especially for deep-seated tumors, hyperthermia applied by interstitial applicators proved to be effective as an adjuvant therapy with brachytherapy. An example from clinical routine is shown in Figure 1.
When designing interstitial antennas, the main objectives are to deposit energy in a well-defined tumor volume in order not to damage normal tissue, and also to achieve a good impedance match.

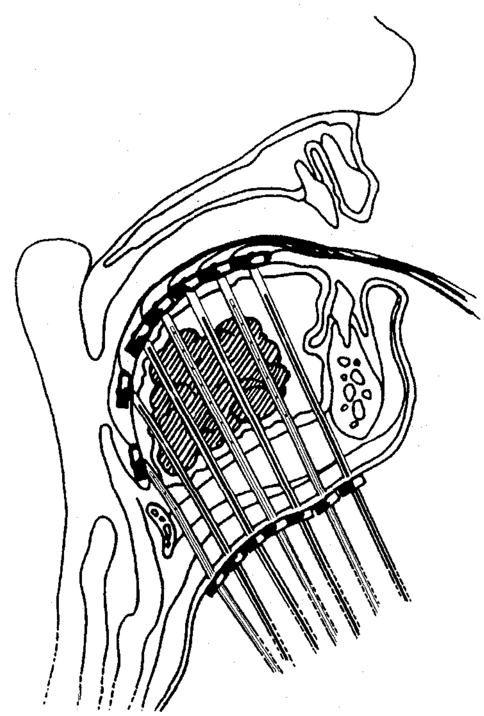

Figure 1: *Hyperthermia treatment of tongue base cancer using interstitial microwave applicators (discussed here) and invasive thermometry.*

Several attempts have been made to analytically calculate the EM-field in the vicinity of such an antenna [2], [3]. Because of the complicated structure of interstitial antennas, together with surrounding catheter, a lot of simplifications have been necessary to perform calculations.

TU 4E

CH3577-4/95/0000-0307$01.00 © 1995 IEEE

It is the purpose of this paper to avoid these simplifications and to model interstitial antennas and catheters as realistically as possible and then to apply numerical calculations. This is done using the field evaluation program **MAFIA** (**MA**xwell's equations using the **F**inite **I**ntegration **A**lgorithm) [4].

The result is a precise pattern of the E-field distribution inside the coaxial line as well as in the catheter, and, of course most interesting, in the lossy tissue. From these field distributions both SAR-distributions and standing wave patterns inside the coaxial line, and therefore the impedance match, can easily be derived.

MODEL AND SIMULATIONS

The rotary symmetry of the applicator can be favourably used to apply a quasi - 2D - simulation. Half of the structure is shown in Figure 2 (not to scale).

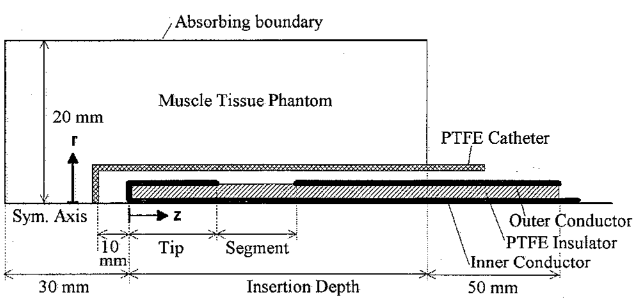

Figure 2: *Model of interstitial applicator with catheter in muscle phantom.*

The applicator consists of a semi-rigid coaxial cable with an outer diameter of 1.2 mm. The applicator is short-circuited at its tip and has a 'radiating' segment of 20 mm in the example given here. It is put into a teflon catheter with an outer diameter of 1.8 mm and the whole applicator is immersed in a muscle tissue phantom (permittivity $\varepsilon_r = 50$, conductivity $\sigma = 1.5$ S/m). Losses in the coaxial cable as well as in the catheter are neglected in the simulation, in fact they are much smaller than those in the muscle tissue. The model is completed by absorbing boundaries at a distance of 20 mm from the symmetry axis. Details about the generation of meshes in the model and about the time-domain algorithms ('solvers') cannot be given here. Simulations have been performed on HP 720 workstations.

RESULTS

The simulated fields inside the semi-rigid cable are used to calculate the frequency dependent reflection of the applicators. These data are compared with measurements accomplished with a Wiltron 360 ANA (Figure 3). The fine structure of the measured curve is mainly due to an antenna connector, which was not included in the calibration procedure of the network analyzer.

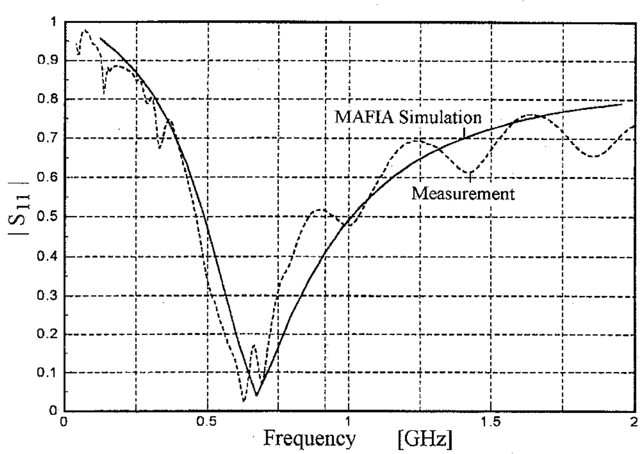

Figure 3: *Measured and calculated |S11(f)| of an interstitial applicator.*

An example of the field and power distributions in the muscle tissue is given in Figure 4.

Figure 4a gives a momentary view of the electric field in muscle tissue at a frequency of 915 MHz. The arrows indicate the direction of the field and its strength at the place where the arrows start.

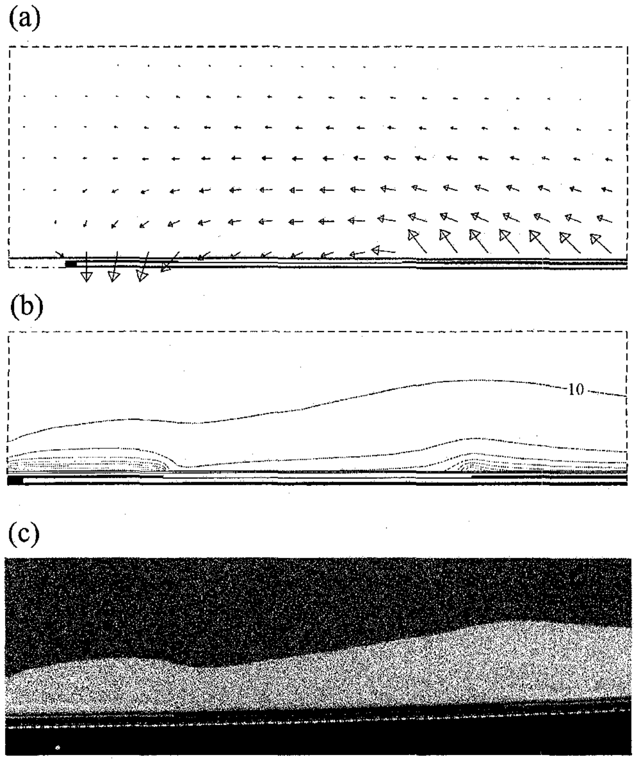

Figure 4: *Calculated E-field (a) and SAR distribution (b and c) of an interstitial applicator.*

Figure 4b shows a plot of equi-SAR contour lines from a maximum of 100 % declining by steps of 10 %.

The same is given in a false colour plot in Figure 4c. Results given in Figure 4 are compared with experimental data from SAR measurements with a computer controlled 3-axis scanning system, where E-field probes are driven by automatic stepper motors in a liquid muscle phantom. The experimental setup is shown in Figure 5.

Experimental results of 3D-SAR-measurements are shown in Figure 6.

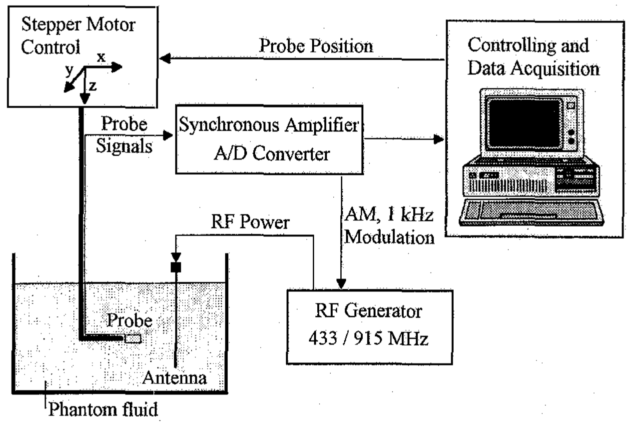

Figure 5: *SAR Measurement Setup.*

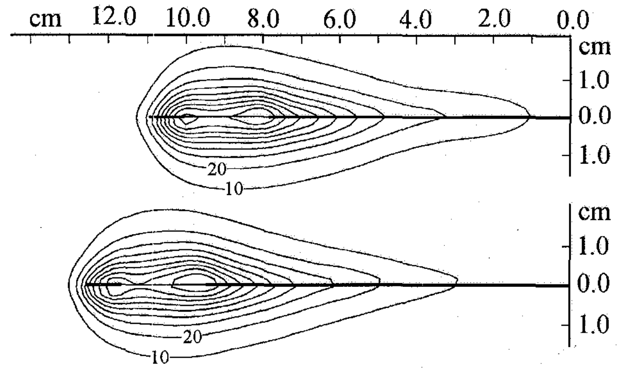

Figure 6: *Measured relative SAR-distributions of clinically used interstitial applicator at different insertion depths: 11cm and 13 cm.*

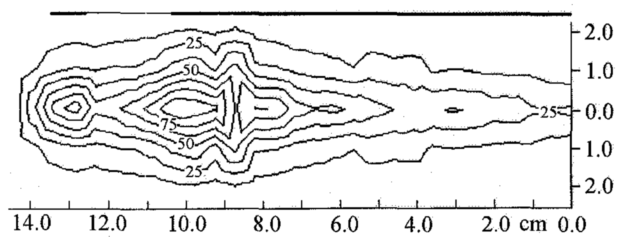

Figure 7: *Measured relative SAR-distribution of an interstitial applicator at 13 cm insertion depth using the 'power-pulse' technique [5].*

Simulation results were also verified by measuring the changes in temperature at known points in a gel muscle phantom [6] following a brief period of heating at high power ("power-pulse" technique) [5].

Comparable SAR-data is directly derived from this procedure and plotted in Figure 7.

CONCLUSIONS

The described simulation procedure allows a quick and precise evaluation of applicators for interstitial microwave hyperthermia. The most important feature is the SAR-distribution around the applicator, however, also the impedance match can be verified.

A few important conclusions are the following:

- The specification of appliators alone makes no sense. The whole system applicator - catheter - lossy tissue has to be considered.
- Insertion depth is a critical parameter when using conventional applicators. Therefore, triaxial applicators are desirable [7].
- The applicators under investigation show strong radial E-field components at their tip ('end-fire' characteristic) [8]. In many cases these strong field gradients cannot be verified experimentally (see Figure 6) because field probes normally integrate signals over several millimeters.

REFERENCES

[1] **J.W. Strohbehn**, **T.C. Cetas** and **G.M. Hahn**. "Special Issue on Hyperthermia and Cancer Therapy - Guest Editorial." *IEEE Trans. Biomed. Eng.* **31**(1), 1 (1984).

[2] **R.W.P. King**, **B.S. Trembley** and **J.W. Strohbehn**. "The Electromagnetic Field of an Insulated Antenna in a Conducting or Dielectric Medium." *IEEE Trans. Microwave Theory Tech.* **31**(7), 574 (1983).

[3] **M.F. Iskander** and **A.M. Tumeh**. "Design Optimization of Interstitial Antennas." *IEEE Trans. Biomed. Eng.* **36**(2), 238 (1989).

[4] **Weiland et al.** "Finite Integration: Ein universell anwendbares Verfahren zur Berechnung elektromagnetischer Felder." *VDE-Fachbericht* **45**, 109 (1993).

[5] **J. W. Hand** and **J.R. James (Eds.)**. "Physical Techniques in Clinical Hyperthermia", Research Study Press, Letchworth, England, 1986.

[6] **C.K. Chou**, **G.W. Chen**, **A.W. Guy** and **H.L. Kenneth**. "Formulas for Preparing Phantom Muscle Tissue at various Radiofrequencies." *Bioelectromagnetics* **5**, 435 (1984).

[7] **W. Hürter**, **F. Reinbold** and **W.J. Lorenz**. "A Dipole Antenna for Interstitial Microwave Hyperthermia." *IEEE Trans. Microwave Theory Tech.* **39**(6), 1048 (1991).

[8] **G. Cerri**, **R. de Leo** and **V.M. Primiani**. " Thermic End-Fire Interstitial Applicator for Microwave Hyperthermia." *IEEE Trans. Microwave Theory Tech.* **41**(6/7), 1135 (1993).

ACKNOWLEDGEMENTS

This work was financially supported by the Deutsche Forschungsgemeinschaft (DFG): Fi 371/2-1 and Se 525/4-2, by the Sofie Wallner Foundation Erlangen and by the Johannes and Frieda Marohn Foundation at the University of Erlangen - Nürnberg.